

KECK OBSERVATIONS OF THE YOUNG METAL-POOR HOST GALAXY OF THE SUPER-CHANDRASEKHAR-MASS TYPE IA SUPERNOVA SN 2007IF

M. CHILDRESS^{1,2}, G. ALDERING¹, C. ARAGON¹, P. ANTILOGUS³, S. BAILEY¹, C. BALTAY⁴, S. BONGARD³, C. BUTON⁵, A. CANTO³, N. CHOTARD⁶, Y. COPIN⁶, H. K. FAKHOURI^{1,2}, E. GANGLER⁶, M. KERSCHHAGGL⁵, M. KOWALSKI⁵, E. Y. HSIAO¹, S. LOKEN¹, P. NUGENT⁷, K. PAECH⁵, R. PAIN³, E. PECONTAL⁸, R. PEREIRA⁶, S. PERLMUTTER^{1,2}, D. RABINOWITZ⁴, K. RUNGE¹, R. SCALZO^{4,11}, R. C. THOMAS⁷, G. SMADJA⁶, C. TAO^{9,10}, B. A. WEAVER¹², AND C. WU³

Submitted to ApJ November 9, 2010; accepted March 10, 2011

ABSTRACT

We present Keck LRIS spectroscopy and *g*-band photometry of the metal-poor, low-luminosity host galaxy of the super-Chandrasekhar mass Type Ia supernova SN 2007if. Deep imaging of the host reveals its apparent magnitude to be $m_g = 23.15 \pm 0.06$, which at the spectroscopically-measured redshift of $z_{\text{helio}} = 0.07450 \pm 0.00015$ corresponds to an absolute magnitude of $M_g = -14.45 \pm 0.06$. Galaxy *g*–*r* color constrains the mass-to-light ratio, giving a host stellar mass estimate of $\log(M_*/M_\odot) = 7.32 \pm 0.17$. Balmer absorption in the stellar continuum, along with the strength of the 4000Å break, constrain the age of the dominant starburst in the galaxy to be $t_{\text{burst}} = 123^{+165}_{-77}$ Myr, corresponding to a main-sequence turn-off mass of $M/M_\odot = 4.6^{+2.6}_{-1.4}$. Using the R₂₃ method of calculating metallicity from the fluxes of strong emission lines, we determine the host oxygen abundance to be $12 + \log(O/H)_{\text{KK04}} = 8.01 \pm 0.09$, significantly lower than any previously reported spectroscopically-measured Type Ia supernova host galaxy metallicity. Our data show that SN 2007if is very likely to have originated from a young, metal-poor progenitor.

Subject headings: supernovae: individual – SN 2007if, supernovae: general, galaxies

1. INTRODUCTION

Type Ia Supernovae (SNe Ia) are vital cosmological tools for measuring the expansion history of the Universe (Perlmutter et al. 1999; Riess et al. 1998), as their luminosities show low intrinsic dispersion (~ 0.35 mag), making them ideal as distance indicators. Outliers from the typical luminosity distribution present an opportunity to explore the underlying physical mechanism in these systems, and provide a critical cross-check for possible “contamination” of future high-redshift SN Ia surveys focusing on the normal SNe Ia. Recently a potential new subclass of exceptionally overluminous SNe Ia has been discovered, starting with the prototype SN2003fg (SNLS-03D3bb Howell et al. 2006), fol-

lowed by SN 2007if (Scalzo et al. 2010; Yuan et al. 2010) and SN2009dc (Tanaka et al. 2010; Yamanaka et al. 2009; Silverman et al. 2011; Taubenberger et al. 2010), and potentially SN2006gz (Hicken et al. 2007).

The generally accepted scenario for the production of a SN Ia is the total disruption of a carbon-oxygen (CO) white dwarf (WD) by thermonuclear runaway as accretion from a binary companion drives it toward the Chandrasekhar mass (M_{Ch}). In the single-degenerate scenario (SD; Whelan & Iben 1973), the WD accretes material from a less-evolved companion, either a main-sequence or red giant star (e.g. Hachisu, Kato, & Nomoto 2008). In the double-degenerate scenario (DD; Iben & Tutukov 1984), two WDs coalesce following orbital decay from gravitational radiation. Howell et al. (2006) were the first to suggest that this new subclass of overluminous SNe Ia are likely the product of super-Chandrasekhar-mass (SC) progenitors systems where substantially more material than M_{Ch} undergoes thermonuclear runaway, producing more ^{56}Ni (see, e.g., Raskin et al. 2010) and resulting in a much more luminous explosion. This interpretation is difficult to reconcile with the traditional SN Ia progenitor scenarios in which the SN itself is triggered as the WD approaches M_{Ch} . In the SD scenario where accretion onto the WD is posited to be steady and stable, an accumulation of significantly more mass than M_{Ch} is highly unlikely (Piro 2008). In the DD scenario, the merger of two WDs whose total mass exceeds M_{Ch} (even by a significant amount) is a natural occurrence, and has made this scenario a favored framework for interpreting the origin of super-Chandrasekhar SNe Ia. There are concerns, however, that the merger of two WDs could result in accretion-induced collapse rather than thermonuclear runaway (e.g. Nomoto et al. 1995). Independent constraints on the probable progenitor properties of SC SNe Ia are therefore critical for unraveling the mystery surrounding these exceptional SNe.

SN 2007if is particularly interesting among this new sub-

¹ Physics Division, Lawrence Berkeley National Laboratory, 1 Cyclotron Road, Berkeley, CA, 94720

² Department of Physics, University of California Berkeley, 366 LeConte Hall MC 7300, Berkeley, CA, 94720-7300

³ Laboratoire de Physique Nucléaire et des Hautes Énergies, Université Pierre et Marie Curie Paris 6, Université Paris Diderot Paris 7, CNRS-IN2P3, 4 place Jussieu, 75252 Paris Cedex 05, France

⁴ Department of Physics, Yale University, New Haven, CT, 06250-8121

⁵ Physikalisches Institut, Universität Bonn, Nußallee 12, 53115 Bonn, Germany

⁶ Université de Lyon, 69622, France; Université de Lyon 1, France; CNRS/IN2P3, Institut de Physique Nucléaire de Lyon, France

⁷ Computational Cosmology Center, Computational Research Division, Lawrence Berkeley National Laboratory, 1 Cyclotron Road MS 50B-4206, Berkeley, CA, 94611

⁸ Centre de Recherche Astronomique de Lyon, Université Lyon 1, 9 Avenue Charles André, 69561 Saint Genis Laval Cedex, France

⁹ Centre de Physique des Particules de Marseille, 163, avenue de Luminy - Case 902 - 13288 Marseille Cedex 09, France

¹⁰ Tsinghua Center for Astrophysics, Tsinghua University, Beijing 100084, China

¹¹ Skymapper Fellow, current address: Research School of Astronomy & Astrophysics, Mount Stromlo Observatory, The Australian National University, Cotter Road, Weston ACT 2611 Australia

¹² New York University, Center for Cosmology & Particle Physics, 4 Washington Place, New York, NY, 10003

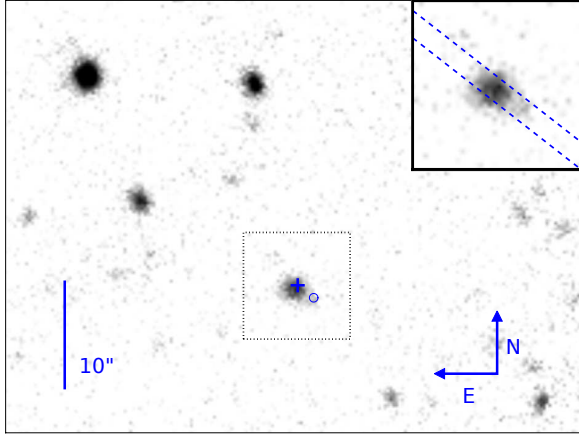


FIG. 1.— Keck LRIS image of HOST07if. The blue cross denotes the location of the supernova. For reference, the “bright” field star in the upper left has magnitude $m_g = 21.1$. The area immediately around HOST07if, denoted by the dotted box, is shown in the upper right inset along with the slit location shown as the dashed lines. The high-redshift background galaxy appears just to the southwest of HOST07if, and its location is marked by the thin blue circle.

class of probable super-Chandrasekhar SNe Ia, as it has been shown to be the most luminous SN Ia ever discovered, with a peak V -band magnitude of $M_{V,07if} = -20.4$ (Scalzo et al. 2010) – nearly a full magnitude brighter than the average SN Ia luminosity of $M_{V,Ia} \sim -19.5$ (Leibundgut 2000). SN 2007if is also interesting for its extremely faint host galaxy ($M_g \sim -14.5$), which we will show below is the lowest-measured metallicity SN Ia host galaxy known. SN 2007if was discovered by the ROTSE-III supernova search (Akerlof et al. 2007) on 2007 August 16.3 UT, and independently by the Nearby Supernova Factory (SNfactory, Aldering et al. 2002) as SNF20070825-001 on 2007 August 25.4 UT (see Scalzo et al. 2010, for details). Located at $\alpha_{2000} = 01:10:51.37$, $\delta_{2000} = +15:27:39.9$, SN 2007if showed no apparent host in search reference images, or in images from the Sloan Digital Sky Survey (SDSS; York et al. 2000). Our deep co-add of NEAT + Palomar-QUEST search data showed a potential host at $m_i \approx 23.3 \pm 0.4$ (Nugent 2007), which at the estimated redshift of SN 2007if would make its host galaxy (hereafter HOST07if) one of the faintest SN Ia hosts ever discovered, suggesting very low metallicity.

In this paper we present observations of HOST07if that confirm its exceptionally low metallicity and establish its luminosity-weighted age. In §2 we present our photometry and spectroscopy, then describe the derivation of gas-phase metallicity and stellar mass and age for HOST07if in §3 and §4, respectively. In §5 we describe cross-checks performed to inspect potential biases or systematic effects in our analysis. We discuss our results in the context of SN Ia hosts and their implications for SN Ia progenitor scenarios in §6. §7 presents our conclusions. Throughout this paper we employ a standard Λ CDM cosmology of $H_0 = 70$ km/s Mpc $^{-1}$, $\Omega_m = 0.3$, and $\Omega_\Lambda = 0.7$.

2. OBSERVATIONS

HOST07if was observed with the Low Resolution Imaging Spectrometer (LRIS, Oke et al. 1995) on the Keck I 10-m telescope on Mauna Kea on 2009 August 23 and 24 UT. We employed the Keck-I atmospheric dispersion corrector (ADC; Phillips et al. 2006). On 2009 August 23.6 five exposures

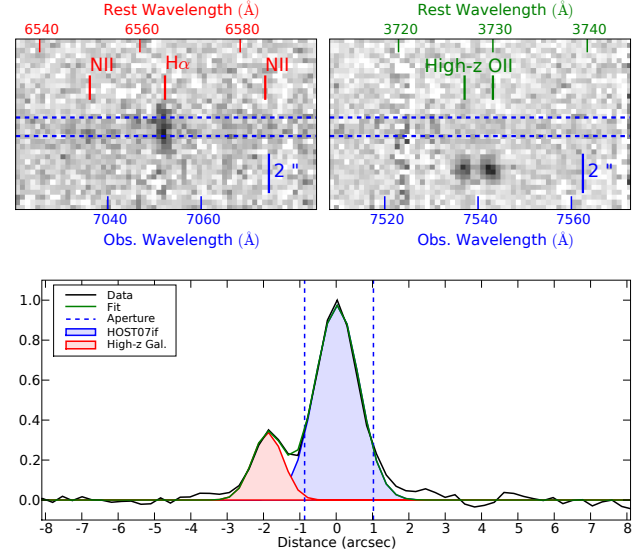


FIG. 2.— *Top*: Portions of the 2D sky-subtracted spectrum image showing (left) the strong $H\alpha$ feature of HOST07if at $\lambda = 7051 \text{ \AA}$ corresponding to $z = 0.074$ (note the distinct absence of [NII] $\lambda\lambda 6548, 6584$), and (right) the [OII] $\lambda\lambda 3727, 3730$ feature of the high- z background galaxy at $\lambda\lambda 7357, 7543 \text{ \AA}$ corresponding to $z = 1.02$. *Bottom*: Wavelength-collapsed object profiles in g -band, showing our two-Gaussian fit to HOST07if and the high- z background galaxy, and the extraction aperture chosen for the HOST07if spectrum. Note the possible contamination from the high- z galaxy is extremely small.

of 100 s duration were obtained in imaging mode using the blue camera of LRIS equipped with a g -band filter. The images were dithered to allow rejection of cosmetic defects, cosmic rays, and to provide image coverage across the detector gap. These images were combined to form a deep image of HOST07if and assess the potential for spectroscopic observation. On the following night (2009 August 24.6 UT) five additional imaging exposures of 100 s duration were obtained in g -band to provide additional photometric depth, then the target was aligned on the slit in imaging mode and the instrument configured for spectroscopic observations. The blue side was configured with the 600 l/mm grism blazed at 4000 \AA , covering 3500–5600 \AA , and on the red side the 900 l/mm grating blazed at 5500 \AA was employed, covering 5500–7650 \AA . The D560 dichroic beamsplitter was used, and no order-blocking filters were necessary. A 1'' slit was oriented at a position angle of 128° along the apparent major axis of HOST07if, which fortuitously was only a few degrees away from the parallactic angle. Our final co-added LRIS image for HOST07if is shown in Figure 1, along with an overlay of the slit. Analysis of the acquisition and slit images show HOST07if to be aligned on the center of the slit to within 1 pixel ($0''.27$). The chosen slit gave resolutions of $\lambda/\Delta\lambda \sim 1000$ (4.4 \AA) and ~ 1600 (4.1 \AA) for the blue and red sides, respectively. Four spectroscopic exposures of 900 s duration were obtained, starting at airmass 1.00 and ending at airmass 1.02. The Keck-I ADC was employed, so we expect no chromatic slit loss due to atmospheric differential refraction. Processing of the photometry and spectroscopy are described below.

2.1. Spectroscopy

The LRIS spectra were reduced in IRAF¹³ using standard techniques. Overscan subtraction was performed for each of the four amps, and the data were mosaiced to form individual two-dimensional frames with data from each amp scaled by its gain. We subtracted bias frames from these data, removed cosmic rays using `LA Cosmic` (van Dokkum 2001), and removed pixel variations in detector efficiency by dividing images by wavelength-normalized flat field dome lamp exposures. The two-dimensional wavelength solution for the blue channel was derived from nightly arc lamp exposures with a linear shift in wavelength applied by measuring the [OI] $\lambda 5579$ atomic night sky line. This linear shift was verified by cross-correlation of the sky spectrum with a high-resolution night sky spectrum from Hanuschik (2003). For the red channel, two-dimensional wavelength solutions for object exposures were derived from night sky lines in the object exposures, while for standard stars we used nightly arc lamp exposures with a wavelength shift determined from [OI] $\lambda\lambda 6300, 6364$ sky lines. Object spectra were reduced to one dimension using the IRAF function `apall`, and nightly flux calibrations were derived from standard stars observed at appropriate ranges of airmass. Telluric absorption features were then removed using the nightly standard star spectra. Finally, the spectrum was corrected for observer motion with respect to the heliocentric frame, and the Galactic reddening of the spectrum was corrected using the Cardelli, Clayton, & Mathis (1989) law and the value $E(B-V) = 0.079$ (Schlegel, Finkbeiner & Davis 1998).

The two-dimensional spectrum of HOST07if showed the presence of a background galaxy separated from HOST07if by $1''.9$ and displaying a strong [OII] $\lambda\lambda 3727, 3730$ doublet at $\lambda\lambda 7537, 7543$ Å, corresponding to $z = 1.02$. Correction for this object in photometric measurements will be described below. We show portions of the background-subtracted 2D red side spectroscopy image in the top panel of Figure 2 to show the offending emission lines from the high- z object. The lower panel of the same figure shows the wavelength-collapsed spatial profile of the 2D blue side spectroscopy image along with the chosen extraction aperture. Based on profile fits to the two objects, we estimate the possible contamination of the extracted HOST07if spectrum by the high- z object to be less than 0.5% at all wavelengths (except at the high- z [OII] doublet position, which does not affect any emission line measurements for HOST07if).

2.2. Photometry

LRIS blue channel photometry was processed in IRAF. Overscan subtraction and mosaicing were performed in the same manner as for the spectroscopy, except that blank pixels were inserted between data from the two detectors to account for the physical gap between the two chips. The images were flat-fielded using g -band dome flats taken earlier in the night. Astrometric solutions were derived using `WCSTools` (Mink 2006), then refined using `SCAMP` (Bertin 2006) matching to 2MASS (Skrutskie et al. 2006). Individual exposures were combined with `SWARP` (Bertin et al. 2002) using median addition, and with proper de-weighting of the detector gap regions and weighting of images by exposure time. With the 5×100 s exposures of 2009-08-23 UT, 5×100 s exposures

of 2009-08-24 UT, and the 4×60 s exposures used for target alignment, the total imaging time at the target location is 1240 s.

The photometric zeropoint for the target was derived by matching objects in the field to SDSS (York et al. 2000) photometry. We extracted magnitudes for all objects in the field using `SExtractor` (Bertin & Arnouts 1996) using the `MAG_AUTO` output parameter, which measures the flux inside an elliptical Kron-like aperture. We then matched objects in our field to the SDSS DR7 (Abazajian et al. 2009) `PhotoObjAll` g -band model magnitudes, ensuring the photometry was clean and the objects were primary targets (`mode=1`). Given the depth of the LRIS imaging, targets brighter than $m_g \sim 16.5$ saturated the detector, so we chose the bright magnitude limit of our catalog matching to be $m_g \sim 17.0$. The SDSS g -band completeness limit is estimated at $m_g \sim 22.2$ with deviation from Pogson magnitudes beginning at about $m_g \sim 22.6$ (Stoughton et al. 2002), so we conservatively chose a magnitude limit of $m_g \sim 22.0$ for our catalog matching. We therefore calculate the photometric zeropoint using the error-weighted mean of $N = 20$ objects between $17.0 < m_g < 22.0$ and find $m_{zp} = 32.59 \pm 0.04$.

The raw instrumental g -band magnitude for HOST07if was observed to be $m_{g,inst} = -9.38 \pm 0.03$. Combined with the SDSS zeropoint and error, we determined the raw g -band magnitude of HOST07if as observed with LRIS to be $m_g = 23.21 \pm 0.05$. The Galactic reddening of $E(B-V) = 0.079$ (Schlegel, Finkbeiner & Davis 1998) results in a g -band extinction of $A_g = 0.34$. In our stacked image, HOST07if is blended with the background high-redshift galaxy described above. To account for its contribution to the measured HOST07if flux, we analyze the two-dimensional blue channel spectrum, which was taken during the best seeing conditions of both nights ($\sim 0''.6$) and shows a clear separation of the two objects. We subtract the sky background from the 2D spectrum, apply the flux calibration and multiply by the g -band filter throughput in the wavelength direction, then collapse the 2D spectrum in wavelength along the aperture trace. This effectively provides a high signal-to-noise measurement of the object profiles along the slit direction in g -band. We then fit this 1D profile with two Gaussians; the data and fit are shown in Figure 2 along with the chosen aperture. The center of both objects fall inside the slit and the seeing was smaller than the slit width, so we predict that the flux within the slit satisfactorily preserves the flux ratio between the two objects. The ratio of the flux of the high- z galaxy to HOST07if in g -band is $F_{\text{high-}z}/F_{\text{HOST07if}} = 0.27 \pm 0.02$, with a separation of $1''.9$. This results in a correction to the observed magnitude of HOST07if of $\Delta m_g = -0.26 \pm 0.02$. Finally we include the known offset between the SDSS and AB magnitude systems (Stoughton et al. 2002) of $m_{g,AB} = m_{g,SDSS} + 0.02$. To derive the rest-frame g -band magnitude, we perform a K-correction (Nugent, Kim, & Perlmutter 2002) using the g -band filter throughput and the HOST07if spectrum, finding $K_g = -0.002$. The reddening, object overlap, SDSS-AB offset, and K-correction effects result in a final rest-frame g -band magnitude of HOST07if of $m_g = 23.15 \pm 0.06$.

To derive the correct distance modulus for HOST07if, we convert the heliocentric redshift derived from nebular emission lines (see §3.1) to the CMB rest frame using the dipole parameters from WMAP5 (Hinshaw et al. 2009) to obtain $z_{\text{CMB}} = 0.07336 \pm 0.00015$. Assuming standard Λ CDM cosmology ($H_0 = 70$ km/s Mpc⁻¹, $\Omega_m = 0.3$, $\Omega_\Lambda = 0.7$), we use

¹³ IRAF is distributed by the National Optical Astronomy Observatory which is operated by the Association of Universities for Research in Astronomy, Inc., under cooperative agreement with the National Science Foundation.

the code of Wright (2006) to calculate a distance modulus of $\mu = 37.60 \pm 0.004$ (note this corrects a transcription error in the calculation of the host absolute magnitude reported in Scalzo et al. 2010, which did not affect any other values reported in that analysis). With the apparent magnitude derived above, this gives HOST07if an absolute g -band magnitude of $M_g = -14.45 \pm 0.06$.

Since the LRIS g -band observations were the only deep late-time photometry of the host (after the SN had fully faded), we analyze the HOST07if spectrum as a source of galaxy color information. We synthesize rest-frame u - g - and r -band magnitudes from the spectrum using the SDSS filter transmissions¹⁴ and obtain effective observer-frame galaxy colors of $g-r = 0.07 \pm 0.04$ mag and $u-g = 0.67 \pm 0.03$ mag. The relative flux calibration of our spectrum is very good, as we measure the synthetic $g-r$ and $u-g$ colors of the night's standard star observations to match those synthesized from calibration spectra to within $\Delta(g-r) < 0.01$ mag and $\Delta(u-g) < 0.01$ mag, primarily driven by noise in the dichroic region. These colors will be used below to derive the galaxy mass-to-light ratio and to inspect possible reddening due to dust.

3. SN 2007IF HOST METALLICITY

Our original objective in observing HOST07if was to secure a host redshift in order to accurately determine the SN 2007if ejecta velocity. This measurement played a key role in establishing the kinetic energy of the explosion and SN 2007if as having a mass greater than the Chandrasekhar limit Scalzo et al. (2010). Fortunately, the final spectrum showed emission in $H\alpha$ and [OII] $\lambda\lambda 3727, 3730$ sufficiently strong to measure a gas-phase metallicity.

3.1. Emission Line Fluxes

Accurate measurement of emission line fluxes in star-forming galaxies requires proper accounting for stellar absorption. To this end we fit the emission line fluxes and stellar background in the HOST07if spectrum simultaneously using a modified version of the IDL routine `linebackfit` from the `idlspec2d`¹⁵ package developed by the SDSS team. This routine allows the user to provide a list of template spectra fit in linear combination with Gaussian emission line profiles. We have modified this code to force the background coefficients to be non-negative and have incorporated the ability to fit for a scaling factor between the blue and red channels of two-arm spectrograph data. For background templates we chose a set of simple stellar populations (SSPs) from the stellar population synthesis code GALAXEV (Bruzual & Charlot 2003, BC03) with a Chabrier (2003) IMF and the same time sampling used for background fitting by Tremonti et al. (2004, T04), which ultimately consists of ten SSPs for each metallicity. We note that the use of Salpeter (1955) IMF templates results in negligible differences to the fitted emission line fluxes, and metallicity difference smaller than the quoted precision of 0.01 dex.

We fit the two LRIS channels simultaneously, with the background templates on each channel convolved to the spectrograph resolution for each channel, namely 4.4 Å and 4.1 Å for the blue and red channels respectively, and fit the cross-channel scaling simultaneously. As with the SDSS spectro-

scopic pipeline, our emission line fitting is done in an iterative fashion. An initial guess of the redshift is used to set the redshift of the background templates, and the spectrum is fit with the widths and redshifts of all lines allowed to float freely. The best redshift is measured from the initial emission line fits, and a second iteration is performed with the redshift of the background templates set to this value. The emission line fluxes are then measured with the line redshifts all fixed to this value. We found the best fit χ^2 was obtained when the background templates were drawn from the $Z = 0.004$ track. The uncertainty in the scaling of the blue and red channels is measured to be $\approx 3\%$, and has a value consistent with those measured for our standard stars. The uncertainties from all fit parameters and their covariances are measured by the fitting code, and emission line flux errors accurately reflect the influence of all fit parameters in their estimation (including the cross-channel scaling). The final emission line fluxes from our best fit are presented in Table 1, and the fit to the spectrum is shown in Figure 3.

TABLE 1
HOST07IF EMISSION LINE FLUXES

Line	Obs. Flux ¹	$F(\lambda)/F(H\beta)^2$
[OII] $\lambda\lambda 3727, 3730$	48.80 ± 10.56	2.44 ± 0.53
$H\beta$	22.29 ± 7.17	1.11 ± 0.36
[OIII] $\lambda 4959$	5.22 ± 2.85	0.26 ± 0.14
[OIII] $\lambda 5007$	15.37 ± 8.38	0.77 ± 0.42
$H\alpha$	57.46 ± 5.30	2.87 ± 0.26
[NII] $\lambda 6548$	0.93 ± 1.25	0.05 ± 0.06
[NII] $\lambda 6584$	2.77 ± 3.72	0.14 ± 0.19
[SII] $\lambda 6717$	7.46 ± 3.52	0.37 ± 0.18
[SII] $\lambda 6731$	6.68 ± 3.71	0.33 ± 0.19

^a Fluxes in units of $10^{-19} \text{ ergs} \cdot \text{cm}^{-2} \cdot \text{s}^{-1}$

^b $F(H\beta) \equiv F(H\alpha)/2.87$; see text for details.

The emission lines from our spectrum of HOST07if provide a formal redshift and uncertainty of $z_{\text{lines}} = 0.074500 \pm 0.000010$ in the heliocentric frame. This value is slightly different from the value we quoted in Scalzo et al. (2010), and reflects a more thorough treatment of the spectrum wavelength solution. Additionally, we calculate the contribution of our wavelength solution to the redshift error budget to be $\Delta z_{\text{wsol}} \approx 2.5 \times 10^{-5}$. Because our object has extent smaller than the slit, the dominant source of redshift error from our data comes from the centering of the object on the slit. As stated above, we measure this error to be no more than 1 pixel, which corresponds to a redshift error of $\Delta z_{\text{slit}} \approx 1.5 \times 10^{-4}$ at $H\alpha$, the line which best constrains the redshift. Thus we estimate the final heliocentric redshift and error for HOST07if to be $z_{\text{helio}} = 0.07450 \pm 0.00015$.

The Balmer emission line fluxes are typically used to estimate intrinsic reddening in galaxies by comparison to the Case B recombination value of $F(H\alpha)/F(H\beta) = 2.87$ at a temperature of $T = 10,000\text{K}$ (Osterbrock & Ferland 2006). This value is well within the 1σ estimate from our measured emission line fluxes (0.62 in the cumulative probability function), but is poorly constrained due to the relatively low S/N of our spectrum. We therefore will report results derived under the assumption of *no intrinsic extinction*. Later, in §5.1, we show that this assumption is supported by multiple facets of the data themselves, and even in the worst case scenario of leaving reddening unconstrained has negligible impact on our final results.

¹⁴ The SDSS filter transmissions are available at <http://www.sdss.org/dr7/instruments/imager/index.html>.

¹⁵ http://spectro.princeton.edu/idlspec2d_install.html

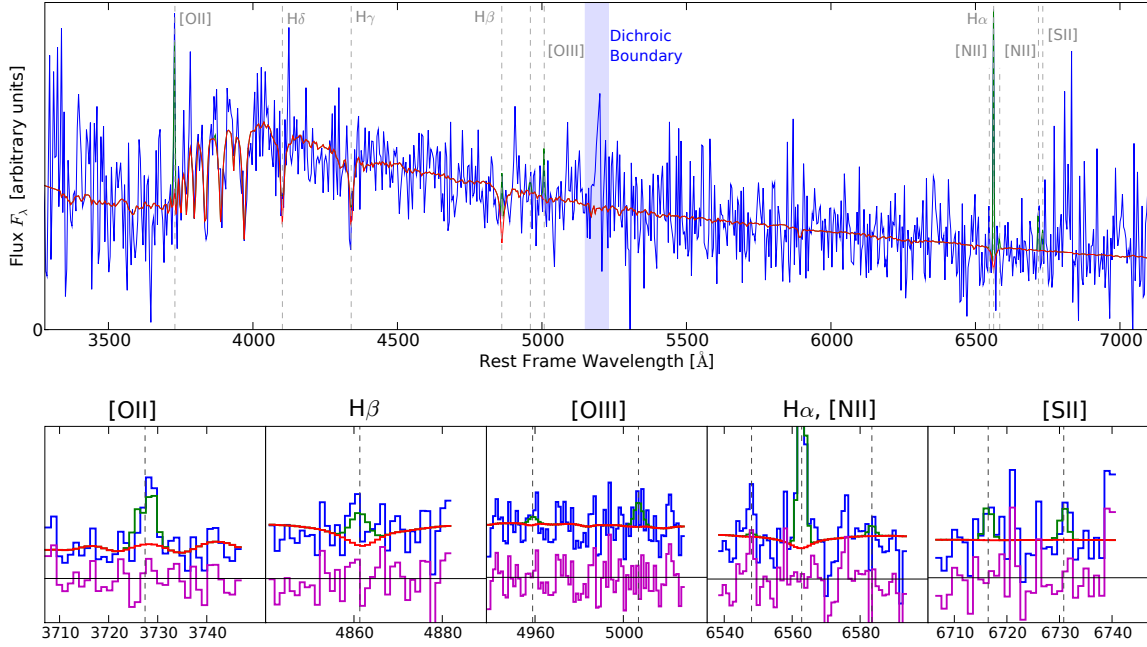


FIG. 3.— *Top*: Spectrum of HOST07if (blue) binned to 4 Å for visual clarity, with fitted background (red) and emission lines (green). *Bottom*: Zoomed fit regions for notable emission lines (unbinned), with fit residuals (magenta).

3.2. Gas-Phase Metallicity

Initial signs that HOST07if is a low metallicity galaxy include the non-detection of [NII] $\lambda\lambda 6548, 6584$ (below the noise threshold, see value and errorbar in Table 1 and 2D spectroscopic image in Figure 2), the relatively weak [OII] $\lambda\lambda 3727, 3730$ and [OIII] $\lambda\lambda 4959, 5007$ lines (compared to the strong Balmer lines), and of course its low luminosity. Low-metallicity galaxy abundances are ideally determined using the “direct” method whereby the ratio of the auroral [OIII] $\lambda 4363$ line flux to that of the stronger [OIII] $\lambda\lambda 4959, 5007$ lines is used to constrain the electron temperature T_e in the doubly-ionized oxygen (O^{++}) zone ($T_e(OIII)$). Because the auroral line is not detected in HOST07if, and the intrinsically stronger [OIII] $\lambda\lambda 4959, 5007$ lines are only weakly detected, the direct method is untenable here.

The question of appropriate metallicity scales will be addressed later in §5.2, but here we derive the metallicity using the R_{23} method of Kobulnicky & Kewley (2004, hereafter KK04). The ratio R_{23} is double valued with metallicity, and the flux ratio [NII]/ $H\alpha$ is typically used to break the degeneracy and select which “branch” of the R_{23} metallicity calibration is appropriate. For HOST07if, [NII]/ $H\alpha$ indicates the lower metallicity branch, so we employ the lower branch of the KK04 calibration of the R_{23} method as updated by Kewley & Ellison (2008). This method is advantageous because it iteratively calculates the metallicity and ionization parameter.

To derive a tighter constraint on the metallicity of HOST07if, we use the higher S/N $H\alpha$ flux measurement and its error scaled by the fiducial Balmer decrement as proxies for the flux and error of $H\beta$. As stated above, this is consistent with our assumption of no reddening in HOST07if and results in an $H\beta$ flux only 0.25σ different from that measured, but with an error bar $4\times$ smaller. For HOST07if, we

measure a metallicity of $12 + \log(O/H)_{KK04} = 8.01 \pm 0.09$, with an ionization parameter $q = 1.46 \pm 0.48 \times 10^7$. This low value of the ionization parameter is unsurprising given the strength of [OII] $\lambda\lambda 3727, 3730$ and the relative weakness of [OIII] $\lambda\lambda 4959, 5007$. These indicate that the ionizing radiation is dilute and it has been some time since HOST07if’s most recent burst of star-formation (consistent with stellar absorption strengths – see below). We note that [NII] $\lambda\lambda 6548, 6584$ is used to break the R_{23} degeneracy, and our measurement of this line predicts the lower branch at only $\approx 69\%$ probability, since [NII] appears to be below the noise level. If we were to choose the upper R_{23} branch, this would make HOST07if a $> 5\sigma$ outlier on the mass-metallicity relation (T04, Kewley & Ellison 2008), an extremely rare event (see e.g. Peebles et al. 2008). Additionally, [NII]/[OII] at such a high metallicity (Kewley & Dopita 2002) would predict an [NII] $\lambda 6584$ flux strong enough to be detected at $> 8\sigma$.

4. SN 2007IF HOST AGE AND STELLAR MASS

Information about the star-formation history (SFH) of HOST07if is desirable for constraining the age of the SN 2007if progenitor. Spectral indices measured from galaxy stellar spectra can be useful in assessing the mean stellar age, likelihood of recent starburst, and stellar mass-to-light ratios (see e.g. Kauffmann et al. 2003a; Graves & Schiavon 2008; Gallazzi & Bell 2009). To facilitate the inspection of the SFH of HOST07if, we measure several age-sensitive spectral indices from the emission-subtracted spectrum of HOST07if and compared their values to model spectra generated using stellar population synthesis (SPS) techniques. The details of our analysis are as follows.

We measured the strength of several Balmer absorption features according to their standard definition on the Lick system (Worthey et al. 1994; Worthey & Ottaviani 1997) as well as the strength of the 4000 Å break (D4000, Balogh et al. 1999) in the spectrum of HOST07if after removing emission

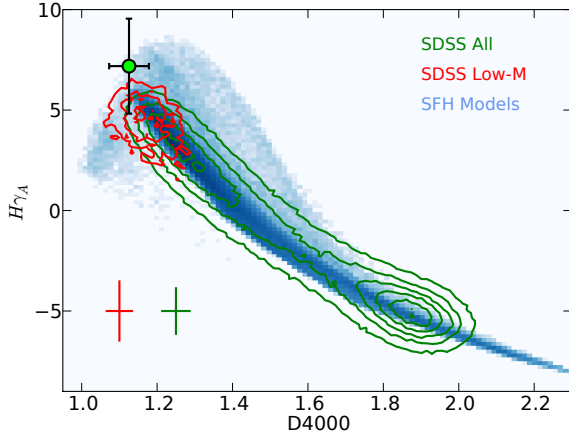


FIG. 4.— Location of HOST07if (green circle) in the $H\gamma_A$ -D4000 plane compared to the library of physically motivated SFHs of GB09 (blue background). Overplotted are index values for SDSS galaxies derived by the MPA-JHU group for the full galaxy mass range (green contours) as well as low mass ($\log(M_*/M_\odot) \leq 9.0$) galaxies (red contours), with median measurement errors shown as the colored crosses in the lower left. Galaxies in the densely-populated band spanning the full range of D4000 have SFHs dominated by continuous star-formation, while the galaxies located away from this band have undergone recent burst of star-formation.

line features as determined in §3.1. Using the formulae of Cardiel et al. (1998), we measure the values and errors reported in Table 2. These indices are known to have strong dependence on stellar age (Vazdekis et al. 2010), with negligible dependence on instrument resolution (and by extension galaxy velocity dispersion). The low D4000 and strong Balmer absorption we measure for HOST07if is indicative of young stellar ages of a few hundred Myr.

TABLE 2
HOST07IF SPECTRAL INDICES

Index	Value
D4000	1.13 ± 0.05
$H\delta_A$	3.50 ± 2.33
$H\gamma_A$	7.19 ± 2.36
$H\beta$	2.34 ± 2.82

To assess the general behavior of the SFH of HOST07if, we generate a library of synthetic galaxy spectra using the BC03 SPS code and a suite of physically-motivated SFHs. We follow the same prescription as Gallazzi et al. (2005) and Gallazzi & Bell (2009, hereafter GB09) to generate models consisting of an exponentially declining continuous SF component superposed with random burst of SF (see GB09 for details). We measured the same spectral indices from our model spectra and plot the location of HOST07if and our model galaxies (blue background) in $H\gamma_A$ -D4000 space in Figure 4. For reference, we also plot the location of SDSS DR7 galaxies whose spectral index values and stellar masses have been measured by the MPA-JHU group¹⁶. The full sample of galaxies between redshifts $0.005 \leq z \leq 0.25$ are shown as the green contour, while low mass ($\log(M_*/M_\odot) \leq 9.0$) galaxies are shown as the red contour, with the median error bars for each quantity (for each subsample) shown as the crosses in the lower left.

¹⁶ <http://www.mpa-garching.mpg.de/SDSS/DR7/>

Kauffmann et al. (2003a) showed the Balmer-D4000 diagram to be an informative parameter space in which to inspect the SFH of star-forming galaxies, and (GB09) extensively analyzed the properties of galaxies in different regions of this diagram (for $H\delta_A$). The dense band of model spectra (dark blue) and the majority of the SDSS galaxies form a sequence of galaxies dominated by continuous star-formation ranging from very old (high D4000, low $H\gamma_A$) to very young (low D4000, high $H\gamma_A$) mean stellar ages. Galaxies whose indices are located away from this band have undergone a strong starburst in the past few hundred Myr.

It is evident that HOST07if is located away from the continuous SFH band in this spectral index parameter space, and is even separated from the majority of low mass galaxies whose mean stellar ages are very young. This indicates that HOST07if underwent a major burst of star formation in its recent past. This is perhaps unsurprising given that HOST07if’s low luminosity implies a low stellar mass, and low mass dwarf galaxies tend to have SFHs characterized by strong yet intermittent bursts of star-formation (Searle & Sargent 1972). In the case of a strong recent starburst, the light from the burst tends to dominate the galaxy spectral energy distribution (SED), which can make it more difficult to constrain the complete galaxy SFH and mass-to-light ratio (GB09). Thus we will proceed by decoupling the recent burst of SF from the remaining SFH of HOST07if. We will first assess the age of the most recent starburst, then investigate the potential presence of older stars in HOST07if.

4.1. HOST07if Burst Stellar Age

To quantify the age of the most recent starburst in HOST07if, we compare the HOST07if spectral indices to those of a library of starburst model spectra generated from the BC03 SPS models. The burst SFHs are simple boxcar functions in time described only by the start and end time of the burst of star-formation. Burst start times are uniformly distributed between 0 and 13.5 Gyr ago, and durations are uniformly distributed between 10 Myr and 1 Gyr. Metallicities were distributed logarithmically between $0.2 < Z/Z_\odot < 2.5$ and distributed as a smoothly decaying function in metallicity ($\propto \log(Z)^{1/3}$) between $0.02 < Z/Z_\odot < 0.2$ (in order to not over-represent low-metallicity bursts).

We derive the luminosity-weighted HOST07if starburst age probability distribution function (PDF) in a probabilistic fashion. For each template galaxy in the burst library, we computed the values of the spectral indices measured in the same way as HOST07if. We then derive each template’s error-normalized separation from HOST07if in this multi-dimensional parameter space defined by the spectral indices as

$$\chi_i^2 = \sum_{\alpha} \left[\frac{a_{\alpha,i} - a_{\alpha,07if}}{\sigma_{a_{\alpha,07if}}} \right]^2 \quad (1)$$

where $a_{\alpha,i}$ is the value of parameter α for template i , and similarly $a_{\alpha,07if}$ and $\sigma_{a_{\alpha,07if}}$ are the value and uncertainty of that same parameter for HOST07if. Each template spectrum is a linear combination of spectra of SSPs of discrete age and metallicity as defined by the BC03 models. We assign a weight to each SSP equal to its integrated optical flux ($3500 \text{ \AA} < \lambda < 10000 \text{ \AA}$), as the brighter SSPs are more likely to drive the spectral features. Thus each template has a luminosity-weighted age PDF that is the product of the template’s coefficients for each SSP multiplied by the luminosity weights

for each SSP (and normalized to unity probability). For each age bin in the HOST07if burst age PDF, each template adds probability to the bin that is a product of the template’s age PDF value for that age bin and the appropriate weighting ($\exp[-\chi_i^2/2]$) for the template’s parameter space separation from HOST07if. The final burst age PDF for HOST07if was renormalized according to the total probability of all templates ($\sum_i \exp[-\chi_i^2/2]$). We use the final HOST07if burst age PDF to derive the median age and $\pm 1\sigma$ errors for the stellar population of HOST07if as derived from the cumulative probability function.

We examined the accuracy of this method by performing the same age measurement with our burst library SEDs where $g-r < 0.5$ mag (thus the youngest subsample of bursts), which we will refer to as the “validation sample”. We tested our method for a variety of combinations of spectral indices, and measured the mean offset from the true value (bias) and dispersion (systematic error) for each combination. In general, the bias was much smaller than the dispersion, and the dispersion decreased as more Balmer indices were added but saturated at the dispersion using the combination of $H\delta$, $H\gamma$, and $H\beta$. The $H\beta$ absorption strength for HOST07if is roughly the same magnitude as the emission equivalent width ($EW(H\beta) = 5.3 \pm 1.5 \text{ \AA}$), so the potential for emission contamination of this index exceeds the reduction in systematic error gained by its inclusion. Additionally, the age sensitivity of the $H\beta$ index is slightly dependent on spectrograph resolution and galaxy velocity dispersion (Vazdekis et al. 2010), whereas the other two Balmer indices are not, and the velocity dispersion of HOST07if is poorly constrained at our spectrum S/N. We thus exclude the $H\beta$ index from our parameter space. We also considered other (non-Balmer) Lick indices, including G4300, but these provided no stronger constraints on the HOST07if age. Given the relative insensitivity of these other indices in the ~ 100 Myr age range found for HOST07if (Vazdekis et al. 2010), this is unsurprising.

The final set of indices used to define the parameter space for template matching was D4000, $H\delta$, and $H\gamma$. We show in Figure 5 the comparison between the median reconstructed stellar age against the median time (green circles) and duration (grey horizontal bars) of the starburst for each model in the aforementioned validation sample. The final mean offset between input and reconstructed age is $\Delta \log(t) = -0.05$ dex with a scatter of 0.06 dex. We thus consider our reconstruction method to be accurate, with a systematic age uncertainty of $\Delta \log(t) = 0.06$.

The final burst age PDF for HOST07if is shown in Figure 6, and we can see that the age constraint is remarkably tight. Our analysis shows the luminosity-weighted stellar age of HOST07if to be $\log(t) = 8.09^{+0.37}_{-0.43} [\text{stat}] \pm 0.06 [\text{sys}]$, or in linear age $t_{\text{burst}} = 123^{+165}_{-77}$ Myr (with the addition of statistical and systematic errors in quadrature). For the BC03 tracks at metallicity $Z = 0.004$ (the closest value to our derived galaxy gas-phase metallicity) this corresponds to a main-sequence turn-off mass of $M/M_\odot = 4.6^{+2.6}_{-1.4}$.

We also investigated the inclusion of optical colors in constraining stellar age, beginning with $g-r$ which is strongly correlated with stellar age and was shown by GB09 to be a good color for constraining M_*/L . The age implied by the HOST07if $g-r$ optical color was somewhat in tension with that implied by the spectral indices ($\log(t) \sim 8.5$ vs. $\log(t) \sim 8.1$). The cause of this discrepancy is likely to be either the presence of some older stars in addition to the re-

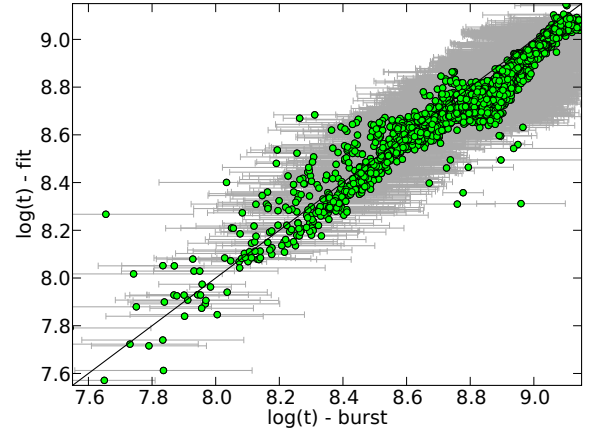


FIG. 5.— Reconstructed starburst age for our selected library galaxies vs. the input time of most recent starburst (green circles), with duration of starburst shown as horizontal grey bars. The scatter about the true value is 0.06 dex.

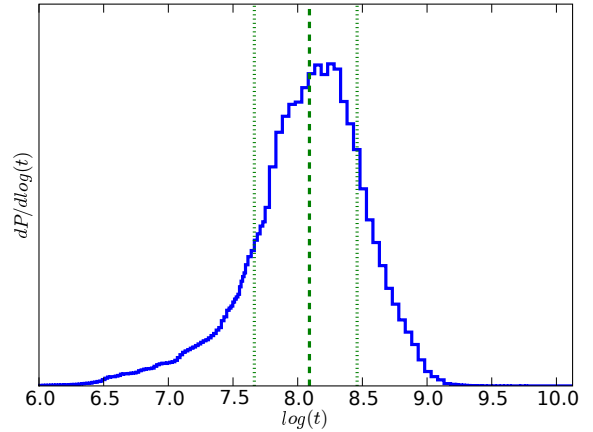


FIG. 6.— Final luminosity-weighted burst age PDF for HOST07if. The solid vertical line represents the median of the cumulative probability distribution, while the two dashed vertical lines represent the 16th and 84 percentile (i.e. 1σ) of the same.

cent burst of star-formation (see §4.2), or intrinsic reddening in the galaxy (see §5.1).

It is worth noting that the distribution of ages and metallicities in the model library has a significant impact on the resultant age PDF. Applying the same method to the GB09-like SFH library used in Figure 4 yields a very differently shaped PDF, and does not successfully recover burst ages for those SFHs with a dominant recent starburst. This is because the manner in which the library SFHs populate the age-metallicity parameter space effectively acts as a prior on the resultant age PDF, whose final form is especially dependent on the way in which different age bins are coupled to one another by the assumed shape of the SFH. Our burst model library employs the simplest possible SFHs (excepting of course a δ -function SFH) and provides an effectively flat and decoupled prior because it populates age and metallicity bins evenly and only couples adjacent age bins with equal weight and over relatively short (< 1 Gyr) timescales.

Finally, we note that our burst age assessment method also provides corroboration of the low metallicity of HOST07if

(measured from emission lines above in §3). In addition to tracking the age distribution of each template, we can inspect the distribution of metallicity tracks used in construction of the templates. Thus we can examine the burst age PDF as a function of metallicity, and derive the integrated probability for each BC03 metallicity track. Doing so yields the following probabilities: 25% for $Z = 0.0004$, 40% for $Z = 0.004$, 17% for $Z = 0.008$, 13% for $Z = 0.02$ (solar), and 5% for $Z = 0.05$. This discrete distribution illustrates the strong preference for lower metallicity tracks despite the relatively flat prior (w.r.t. each track). This is a product of the metallicity sensitivity of the spectral indices used in the data-model comparison, and shows that the stellar spectral features favor a low metallicity in agreement with our measurement of the gas phase metallicity above.

4.2. Old Stars in HOST07if

Perhaps the greatest limitation in our ability to constrain the age of the SN 2007if progenitor is the uncertainty in the amount of old stars in HOST07if. Low-mass dwarf galaxies such as HOST07if are likely to have a bursty SFH (Searle & Sargent 1972) characterized by intense bursts of star-formation separated by extended quiescent periods of reduced SFR (Sánchez Almeida et al. 2008). Such galaxies may have formed the majority of their stars in the distant past (Zhao, Gu, & Gao 2011), so it is critical to investigate the potential amount of old stars in HOST07if.

The bursty nature of the HOST07if SFH is supported by the comparison of the burst star-formation rate (SFR) implied by our age constraint as compared to that implied by the observed $H\alpha$ emission. We showed above that the HOST07if spectrum is dominated by stars of age 123 Myr, and we can make a simple approximation of the mass of stars formed during the burst by multiplying the observed g -band flux by the mass-to-light ratio of our estimated burst age (and metallicity). Doing so yields an approximate mass of $10^7 M_\odot$ of stars formed in the burst, and if we assume this was formed in $t \approx 100$ Myr (likely an extreme over-estimate), we can estimate a rough burst SFR of $SFR_{burst} \approx 0.1 M_\odot \text{ yr}^{-1}$. The presence of $H\alpha$ emission implies some current star-formation, which we can quantify using the formula of Kennicutt (1998) to find $SFR_{H\alpha} = 2.2 \times 10^{-3} M_\odot \text{ yr}^{-1}$. Thus, even our crude estimate of the burst SFR shows the ratio of SFR during the burst to that at the present time to be at least $SFR_{burst}/SFR_{H\alpha} \approx 50$, which implies that the HOST07if SFR is tapering off from its intense value during the recent burst.

To investigate the amount of old stars in HOST07if, we begin by reconstructing the spectrum derived by convolving the burst 2D age-metallicity PDF with the BC03 SSPs. This “reconstructed” stellar spectrum is plotted in the top panel of Figure 7 along with the data and stellar background fit from §3. Remarkably, information from the Balmer absorption features and D4000 alone are enough to reconstruct much of the HOST07if stellar background with high fidelity, especially in the bluer wavelengths. A slight color discrepancy of $\Delta(g-r) \approx 0.11$ mag is evident here, which could be due to dust in HOST07if (see §5.1) or old stars (see discussion below). In the lower panel of the same figure, we show the ionizing flux below the Lyman limit ($\lambda = 912 \text{ \AA}$) for the reconstructed spectrum as compared to the SSP at the age closest to our median age and metallicity closest to our spectroscopic measurement ($Z = 0.004$). We performed a simple calculation of the $H\alpha$ flux that would result from this ionizing flux as-

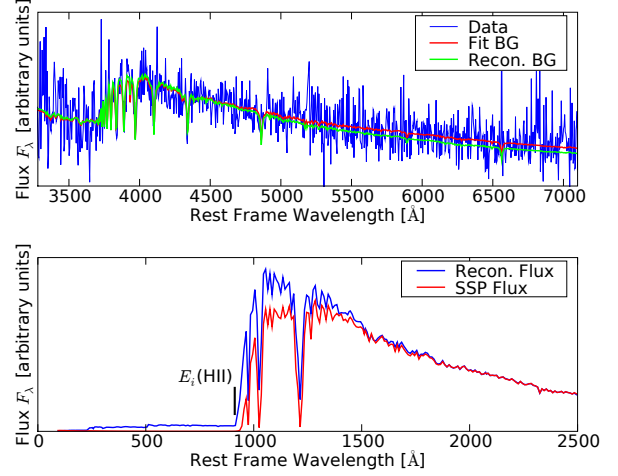


FIG. 7.— *Top*: Comparison of the spectrum reconstructed from the HOST07if age PDF (green) compared to the data (blue) and the background estimate from the emission-line fitting procedure (red). *Bottom*: A comparison of the reconstructed spectrum (blue) and the spectrum of the SSP with age closest to the age estimate for HOST07if. Note the presence of HII ionizing radiation in the reconstructed spectrum while the SSP (as expected) shows none.

suming 45% of ionizing photons eventually generate an $H\alpha$ photon (Donahue, Aldering, & Stocke 1995), and found it to be within a factor of about 2 of the measured value. Thus, our technique not only accurately reproduces the stellar spectrum in the optical regime, but also independently predicts the Balmer emission strength fairly well. This indicates that our age-matching technique is effectively reproducing the tapering SFR in HOST07if, which may indicate we are recovering not only the central burst time, but also some of the morphology of the burst SFH.

We proceed in our investigation of possible old stars in HOST07if by taking our reconstructed burst spectrum as being representative of the true starburst SED. As noted above, the spectrum predicted from our burst PDF is somewhat bluer ($\Delta(g-r) \approx 0.11$ mag) than what we observe for HOST07if, which could be a product of additional old stars. Here we take a conservative approach and explore the implications if the entire color excess arises from an old stellar population. To the burst spectrum we add the SED from an additional mass of old stars injected at a single age ranging from 1 Gyr to 13.5 Gyr. For each age, we fit for the mass of stars that minimizes χ^2 from the $g-r$ and $u-g$ colors, as well as the upper and lower masses that produced a $\Delta\chi^2$ of 1 (i.e. $\pm 1\sigma$) from the optimum value. In Figure 8 (top panel) we plot the best mass (and $\pm 1\sigma$ values) of old stars (normalized to the burst mass) as a function of age, as well as the best fitting χ^2 (middle panel). For reference in this plot, we show the best χ^2 obtainable by reddening the burst spectrum with dust (at $R_V = 3.1$), found to be $\chi^2 = 1.14$ at $A_V = 0.22$ mag. At all ages, the spectral features (D4000, $H\delta_A$, $H\gamma_A$) of the old+burst spectrum differed from the observed values in HOST07if by much less than their measured uncertainties, justifying our approach of examining the starburst and old stellar populations separately.

This test illustrates the aforementioned fact that young bursts of star formation tend to obscure older stellar populations. Half or more of the stars in HOST07if could indeed come from older stars and still be consistent with the observed

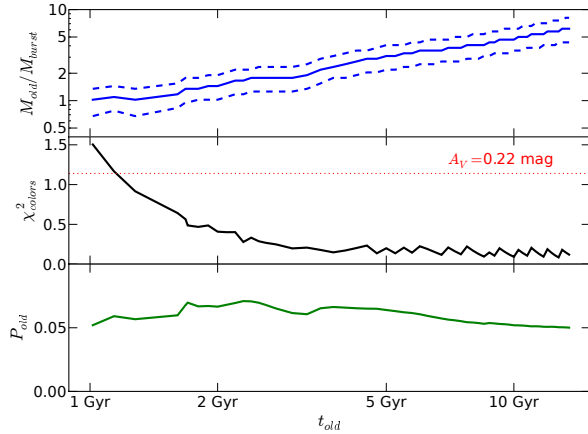


FIG. 8.— *Top:* Best fit value (solid blue line) and $\pm 1\sigma$ values (dashed lines) for mass of old stars at each age that when added to the burst spectrum produce the best matching colors ($g-r$ and $u-g$), scaled to the mass of the burst spectrum. *Middle:* χ^2 of colors for best-fit mass value as a function of age (solid black line), with the best possible χ^2 obtainable by reddening the burst spectrum (dotted red line) which is found at $A_V = 0.22$ mag. *Bottom:* Final probability of SN 2007if arising from old stars injected at a given age, derived from the product of the SN production likelihood with the color-matching likelihood (from the above χ^2 values).

spectral indices and colors, and we can currently only disfavor old stars in HOST07if by making assumptions about the form of its SFH. However, our age measurement technique showed that old stars alone are inconsistent with the observed spectral features of HOST07if, and a significant amount of young stars dominates the galaxy spectrum. Further observational constraints on old stars in HOST07if must wait for additional data, such as deep imaging in the near infrared.

An old stellar population can be the source of SN 2007if only if its reservoir of potential progenitor systems has not been exhausted. Making the simplest assumptions – that the original reservoir of progenitor systems is proportional to initial stellar mass, M_{old} , and that the delay time distribution (DTD) of SN 2007if-like events is not an increasing function of the delay, t_{old} , for populations older than ~ 100 Myr – we can define a maximum relative rate today, given by $(M_{old}/t_{old})/(M_{burst}/t_{burst})$, arising from any ancient burst of star formation. Coupling this relative rate with the best-fit value of M_{old} for each age, and scaling by the χ^2 probability from the color matching, we derive the total probability of SN 2007if having been born from an old stellar population as a function of age. The results are shown in the bottom panel of Figure 8, where one sees that the likelihood of SN 2007if arising from an older stellar population never exceeds about 7% (note that this could be even lower if there is some reddening due to dust). We therefore conclude there is a high likelihood that SN 2007if was born in the recent burst of stars whose age was constrained in §4.1. We note that mathematically this consumption-timescale constraint gives the same relative factor as for old stellar populations distributed equally at multiple ages – where consistency requires a fixed DTD normalization across ages – and then assuming a t^{-1} power law for the DTD. This case is of particular interest because a t^{-1} power law is similar to the DTD observed for normal SNe Ia (Maoz 2010; Barbary et al. 2010), and expected in most DD models.

4.3. HOST07if Stellar Mass

The SPS models used above to constrain the luminosity-weighted age of the HOST07if stellar population can also be used to constrain the HOST07if mass-to-light ratio. Though spectral indices can in principle be used to constrain the mass-to-light ratio (e.g. GB09), the S/N of our spectral indices results in a large uncertainty (~ 1 dex) in the index-based mass-to-light ratio. Instead, a much tighter constraint can be obtained using optical color. We thus compare the $g-r$ color of HOST07if to that of our SFH models, as this color was shown by GB09 to be a good color for constraining mass-to-light ratios.

Which SFH models are appropriate for determining mass-to-light ratios is a deeper question than can be addressed here. Instead we follow the prescription generally favored in the literature, which is to use exponentially-declining SFHs similar to those of Kauffmann et al. (2003a) and GB09. Though the SFHs of dwarf galaxies such as HOST07if are likely to be bursty, a long period of intermittent burst of SF can be well-approximated by a continuous SFH. We thus use the aforementioned suite of model spectra built following the prescriptions of GB09 to constrain the HOST07if mass-to-light ratio using $g-r$ color in the following way. Each model galaxy SED is normalized to $M = 1M_{\odot}$, and we measure the g -band luminosity for each template. Using color-based χ^2 weights, we measure the weighted mean stellar mass of a burst of unit g -band luminosity as:

$$\langle M \rangle = \frac{\sum_i w_i M_i}{\sum_i w_i} \quad (2)$$

and its uncertainty:

$$\sigma_M = \left(\langle M^2 \rangle - \langle M \rangle^2 \right)^{1/2} \quad (3)$$

where the weight $w_j = \exp(-\chi_j^2/2)$ for each template is computed from the template's $g-r$ color χ^2 as:

$$\chi_j^2 = \left[\frac{(g-r)_{HOST07if} - (g-r)_j}{\sigma_{(g-r)_{HOST07if}}} \right]^2 \quad (4)$$

Assuming a solar g -band absolute magnitude of $M_{\odot,g} = 5.15$ (Bell & de Jong 2001), we derive a mass-to-light ratio for HOST07if of $\log(M_*/L)_{model} = -0.50 \pm 0.17$. With the absolute magnitude derived in §2.2 and the aforementioned mass-to-light ratio, this implies a galaxy stellar mass for HOST07if of $\log(M_*/M_{\odot}) = 7.32 \pm 0.17$.

As a comparison, we inspect the mass-to-light ratios for SDSS galaxies as determined by the MPA-JHU team. We find their M_*/L values to be well represented as a linear function in both optical $g-r$ color and more weakly in absolute magnitude M_g . From their data, we estimate the HOST07if mass-to-light ratio to be $\log(M_*/L)_{SDSS} = -0.52 \pm 0.15$, which is consistent with our value within the error bars (as would be expected since our SFH models are essentially the same). In a similar vein, we use the color-based M_*/L formulae (appropriately corrected for our choice of IMF) from Bell & de Jong (2001) along with the color measured from HOST07if to estimate a mass-to-light ratio of $\log(M_*/L) = -0.55$, again consistent with our estimate.

5. ANALYSIS CROSS-CHECKS

We now discuss several cross-checks we performed in order to estimate systematic effects in our parameter estimations.

The possible effects of dust in HOST07if, systematic uncertainties in metallicity scales, and the limitations of our particular choice of stellar population synthesis (SPS) models will be addressed in turn.

5.1. The Effect of Uncertain Reddening

In typical applications the Balmer decrement is used to estimate reddening due to dust and correct emission line metallicity diagnostics. Our detection of $H\beta$ is consistent with no reddening, however it is of sufficiently low S/N that a large range of reddening is allowed by this measurement. Several lines of evidence suggest that the reddening should be low. In Scalzo et al. (2010) we set strong upper limits on the column of Na I, suggesting little enriched material is available in the ISM for the formation of dust. Given that HOST07if is in a post-starburst phase, the HII regions and molecular clouds associated with this burst will have dissipated long ago, and thus it is quite plausible that the extinction limit derived for SN 2007if is not atypical of that for the emitting gas and stars. Because dust requires metals to form, the expected low metallicity based on the low luminosity of HOST07if also leads to the expectation of low extinction. Lee et al. (2009) and Garn & Best (2010) measure the Balmer decrement as a function of galaxy luminosity and do indeed find that low-luminosity galaxies typically have extinction of only $A_V \sim 0.1$.

The emission line fluxes of HOST07if also favor low reddening. Correction for reddening will increase R_{23} and lead to a higher predicted O/H. However, N2O2 ($=[\text{NII}]\lambda 6584/[\text{OII}]\lambda\lambda 3727, 3730$) works in the opposite sense. Indeed, at the lowest metallicities ($12 + \log(\text{O}/H) < 8.1$), N2O2 is expected to saturate at primary N/O nucleosynthesis ratio of $\log(N/O) = -1.43^{+0.07}_{-0.08}$ (Nava et al. 2006), giving $\text{N2O2} = -1.32^{+0.08}_{-0.09}$. Thus, our non-detection of $[\text{NII}]\lambda 6584$ provides an upper limit on N2O2 that can be used to constrain the amount of reddening. In the upper left panel of Figure 9 we show these complementary constraints in the A_V –(O/H) plane. These constraints alone disfavor any reddening greater than $A_V \sim 1.8$, and the metallicity prediction would have been 0.21 dex higher than that derived with fixed $A_V = 0$.

The very blue color and strong Balmer absorption of the stellar continuum in HOST07if place additional constraints on reddening. It was noted above that the reconstructed spectrum from our age-metallicity PDF was slightly bluer (by ~ 0.11 mag in $g-r$ and 0.06 mag in $u-g$, corresponding to a best-fit extinction of $A_V = 0.22$ mag) than the observed color of HOST07if. While this could be caused by reddening due to dust, it could also be indicative of the presence of older stars (see §4.2). However, the Balmer absorption of the HOST07if stellar continuum and its optical colors can be combined to place an *upper* limit on the amount of reddening that is consistent with the observed color of HOST07if. This can be understood as a disagreement between the extreme blue stellar color implied by large reddening and the Balmer absorption strengths; if the reddening was large and HOST07if was intrinsically much bluer, its implied age would be younger and thus its Balmer absorption strengths would have been shallower than observed. We can quantify this constraint by examining the effect of reddening on the $g-r$ and $u-g$ colors of HOST07if and the subsequent agreement with our model spectra used in constraining the burst age. For each value of A_V , we sum the probability of matching to each of the

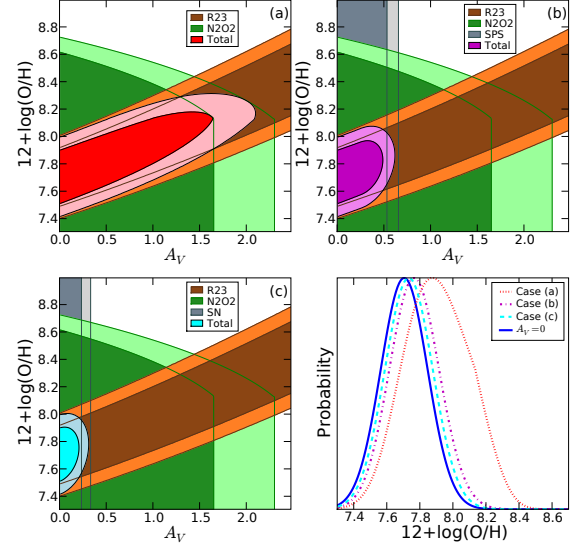


FIG. 9.— *Upper Left*: Two-dimensional probability distribution function of O/H vs. A_V combining constraints from the R_{23} ratio and N2O2 ratio from emissions lines. The two filled contours represent the 1σ and 2σ probability levels for each constraint, with the red and pink contours corresponding to the 1σ and 2σ final combined constraints. *Upper Right*: Same as left, but with additional constraint from SPS matching (see text). Magenta and fuchsia contours are final 1σ and 2σ combined constraints. *Lower Left*: Same as upper left, but with addition of SN reddening constraint from Scalzo et al. (2010). Cyan and light blue contours are final 1σ and 2σ combined constraints. *Lower Right*: Metallicity PDF (marginalizing in A_V) for the three above cases (Case a - emission line constraints only, red dotted line; Case b - emission line plus SPS constraints, magenta dash-dotted line; Case c - emission line plus SN constraints, cyan dashed line) as well as the simple case assuming $A_V = 0$ (blue solid line).

150,000 burst templates using the χ^2 method described above with the $g-r$ and $u-g$ colors included in the χ^2 . Shown in the upper right panel of Figure 9, the A_V PDF from this method shows a sharp drop at $A_V \sim 0.5$. With the constraints from the stellar features added to our PDF, the metallicity we would have measured is only 0.08 dex higher than the $A_V = 0$ value. With the 1σ reddening of $A_V \sim 0.5$, our mass estimate for HOST07if would have increased by ~ 0.3 dex (accounting for both the luminosity and mass-to-light ratio changes), only slightly larger than the measurement error for that quantity.

Finally we show the result of including the SN 2007if reddening constraint of Scalzo et al. (2010) as an assumed constraint on the global host reddening. We show the resultant 2D PDF in the lower left panel of Figure 9, and find that the resultant metallicity would have been 0.02 dex higher than the $A_V = 0$ value. Marginalizing our 2D PDFs in A_V gives the (O/H) PDFs for each scenario described above, and we show these in the lower right panel. The values we reported for each scenario represent the metallicity of maximum likelihood for the PDFs shown. Thus, while there is some uncertainty in the amount of reddening in HOST07if because we cannot strongly constrain the Balmer decrement, ultimately it has little effect on our final results, which robustly show a low metallicity. Additionally, the spectral indices used in our age measurement are measured across short wavelength ranges and thus are relatively insensitive to reddening, making our age estimate also robust against possible reddening in HOST07if.

5.2. Metallicity Calibration

Strong emission-line methods such as the R_{23} method (McGaugh 1991; Zaritsky et al. 1994, KK04) produce oxygen abundance values that are systematically higher than those derived with the direct method by 0.2 – 0.5 dex (Kennicutt, Bresolin & Garnett 2003). In galaxies like HOST07if where [OIII] $\lambda 4363$ is not detected with sufficient S/N but strong line fluxes indicate low metallicity, this poses a challenge for deriving the correct absolute metallicity. Placing our metallicity estimate on the correct absolute scale is subject to the uncertainty as to which metallicity calibration is correct in an absolute sense. This is a subject much debated, and while the final scale remains undecided, Kewley & Ellison (2008) provided an excellent analysis of the discrepancies between various scales and means of converting between them. The scatter in these relations (0.06 dex systematic error, see analysis below) is smaller than the measurement errors from our spectrum. Placement of our measurements on a common scale with those of other SN Ia hosts in the literature suffices for comparison purposes, and will be employed in the discussion of §6.1.

5.3. Systematics in Stellar Population Synthesis

Next, we consider the impact of our particular choice of SPS models. It is a well-known problem that different stellar evolution and population synthesis codes produce different results due to different treatment of uncertain stages of stellar evolution, extinction due to dust, and the IMF (see e.g. Conroy, Gunn, & White 2009). Assessment of the full impact of these uncertainties is beyond the scope of this work, but we inspected the impact of employing a Salpeter (1955) IMF instead of the Chabrier (2003) IMF used in our primary analysis. The age constraint for HOST07if remained unchanged, as the Salpeter IMF increases the amount of low-mass stars (relative the Chabrier IMF) which negligibly affect the spectrum of young starbursts similar to HOST07if which are dominated by bright massive stars. The mass-to-light ratio, however, is ≈ 0.16 dex higher for the Salpeter IMF, again a product of the increased proportion of low mass stars. Thus while our host mass is (as expected) dependent on the IMF chosen, the age constraint is robust against different IMFs.

To place our results in a more general stellar population context, we inspected the stellar spectra catalog of Gunn & Stryker (1983) and measured the Balmer absorption strengths in the same manner as for HOST07if. We then analyzed which single star spectra had the closest absorption strengths to HOST07if, and found the majority of these to be late B-type or early A-type stars. This is consistent with the age and main-sequence turnoff mass derived for HOST07if. Thus we find that our age measurement for the stellar population dominating the light of HOST07if is consistent with single-star spectra, indicating that our results are unlikely to be strongly dependent on the choice of SPS models.

5.4. Summary

In summary, the possible systematic errors or biases on our measurements of the metallicity and age of HOST07if are small compared to measurement errors. Our classification of HOST07if as metal-poor is confirmed for a wide variety of assumptions about reddening by dust in the host, and is true regardless of the metallicity calibration chosen. Our measurement of the young age of the stellar populations in HOST07if is not an artifact of our choice of SPS models or template

SFHs. One important subtlety to note is that our age PDF for the stellar populations in HOST07if does not constitute a direct measurement of the progenitor age of SN 2007if, as the SN progenitor system was drawn from a single epoch in the SFH of its host galaxy. Our estimate of the stellar ages of the host represents the distribution of ages from which the progenitor was drawn, rather than a constraint on the age of the single progenitor system. The statistics of the host age distribution strongly favor a young age for the progenitor system of SN 2007if. Our assertion that HOST07if is young and metal-poor is robust, and serves as appropriate context for considering the properties of the progenitor of SN 2007if.

6. DISCUSSION

In this section we discuss HOST07if in the context of previous SN Ia host galaxy studies, as well as the implications for progenitor scenarios for SN 2007if suggested by our data. Our assumption is that the properties of the host galaxy stellar population are good indicators of the properties of the progenitor system of SN 2007if. We showed above that this argument is statistically sound, as the recent major starburst dominates the galaxy light. Below we will show that our results are consistent with regions of progenitor parameter space believed to produce SNe Ia, and our results thus provide important constraints on what portions of that parameter space are likely to produce super-Chandrasekhar SN Ia.

6.1. Metallicity of SN 2007if host - Comparison to other SN Ia hosts

Metallicity is a key parameter affecting the evolution of SN Ia progenitors. In the SD scenario (Hachisu, Kato, & Nomoto 2008), accretion is stabilized by a strong wind from the WD whose strength is driven by Fe opacity. Lower metallicity decreases the allowable regions of WD mass - orbital period parameter space in which the wind is strong enough to stabilize the accretion (Kobayashi & Nomoto 2009). In general, metallicity will affect the relation between initial main-sequence mass and final WD mass, as well as the time to evolve off the main sequence (Umeda et al. 1999a). For WDs of the same mass, a lower metallicity produces a slightly lower C/O ratio (a product of the aforementioned evolution time effect), which has been proposed as a possible source of the diversity in SN Ia brightnesses (Umeda et al. 1999b).

Placing our metallicity measurement in the context of previously published spectroscopic SN Ia host metallicities requires using a common scale, as different metallicity calibrations produce significantly different results (see the excellent discussion in Kewley & Ellison 2008). To our knowledge, the lowest spectroscopic SN Ia host metallicities to-date are those of SN 1972E at $12 + \log(O/H) = 8.14$ (Hamuy et al. 2000), and SN 2004hw at $12 + \log(O/H) = 8.23$ (Prieto et al. 2008). The original metallicity of the host of SN 1972E is drawn from Kobulnicky et al. (1999), who use the “direct” method to measure the oxygen abundance. As noted above, the “direct” method values are typically lower than strong line values by at least 0.2 dex. Therefore we collected the galaxy emission line fluxes from Kobulnicky et al. (1999) and measured its abundance using the KK04 technique employed for HOST07if, finding $12 + \log(O/H)_{72E, KK04} = 8.35 \pm 0.03$. The metallicities of Prieto et al. (2008) come from SN Ia hosts in the T04 sample, where metallicities were derived in a Bayesian manner by comparing emission line fluxes to photoionization models of Charlot & Longhetti (2001). While the

means to reproduce their metallicity analysis are not available, the absorption-corrected emission line fluxes are available from the MPA-JHU group. Using the fluxes for the host of SN 2004hw, we find $12 + \log(O/H)_{04hw, KK04} = 8.24 \pm 0.03$. After placing all these metallicities on a common scale, our value of $12 + \log(O/H)_{KK04} = 8.01 \pm 0.09$ for the metallicity of HOST07if is $\approx 2\sigma$ lower than the lowest metallicity from these previous samples, and far below the metallicities of typical SN Ia host galaxies.

Interpretation of the metallicity of HOST07if on an absolute scale is subject to the inter-calibration issues described above. The T04 scale is a popular one in the literature, as the mass-metallicity relation they derive is often invoked to use host mass as a proxy for metallicity. As stated above, the algorithm for this scale is not accessible, but we can convert our values to this scale using the conversion formulae of Kewley & Ellison (2008). Doing so yields a metallicity for HOST07if of $12 + \log(O/H)_{T04} = 7.71 \pm 0.14[\text{stat}] \pm 0.06[\text{sys}]$, and for the host of SN 1972E yields $12 + \log(O/H)_{72E, T04} = 8.22$, while the value for SN 2004hw of $12 + \log(O/H)_{04hw, T04} = 8.23$ was derived in the T04 data set. On this scale HOST07if is nearly 3σ lower metallicity than the other SN Ia hosts.

We can place the metallicity of HOST07if on a solar abundance scale by comparing our measurements of the oxygen abundance to the solar value of $12 + \log(O/H)_{\odot} = 8.86$ (Delahaye et al. 2010). On the KK04 scale, HOST07if has metallicity $Z_{KK04} \approx Z_{\odot}/5$, while on the T04 scale it has $Z_{T04} \approx Z_{\odot}/9$. The T04 value is perhaps in better agreement with the stellar metallicity preferred by our template matching (see §4.1) where 40% of the probability is in the $Z = 0.004$ ($Z_{\odot}/5$) track and 25% in the $Z = 0.0004$ ($Z_{\odot}/50$), though the coarse metallicity binning of the BC03 models makes this difficult to quantify precisely. While the absolute scale is somewhat uncertain, the metallicity of HOST07if is significantly sub-solar on several reasonable metallicity scales.

Finally we note that the gas-phase metallicity measured for HOST07if at the present epoch may be higher than the metallicity at the time of the birth of the progenitor of SN 2007if, presumably during the major starburst 123 Myr before the SN. The massive stars formed during that burst have exploded as core collapse SNe and enriched the ISM of HOST07if with their ejecta. Sánchez Almeida et al. (2009) found that dwarf galaxies with bursty SFHs showed gas-phase metallicities enriched by ≈ 0.35 dex (as compared to stellar metallicities) during the periods between bursts of star-formation. Thus the metallicity of the progenitor system of SN 2007if could possibly be even lower than the extremely low gas-phase metallicity measured for HOST07if at the time of the SN itself.

6.2. SNe Ia in low luminosity hosts

SN 2007if is part of a large and continually growing list of unusual SNe Ia discovered in low-luminosity host galaxies. Though low-luminosity galaxies have a higher number density than high-luminosity galaxies due to the steep faint-end slope of the galaxy luminosity function (e.g. Schechter 1976), high-luminosity galaxies retain the majority of stellar mass and thus are likely to produce the large majority of supernovae. Despite this fact, the number of supernovae in low-luminosity hosts is now significant, and includes a number of peculiar SNe such as SN 2007if.

The SN 2002cx-like supernova SN 2008ha (Foley et al. 2009) was found in a faint ($M_B = -18.2$ for $h = 0.7$) irregular galaxy. SN 2002ic (Wood-Vasey et al. 2002; Hamuy et al.

2003; Wood-Vasey, Wang, & Aldering 2004) and SN 2005gj (Aldering et al. 2006; Prieto et al. 2007), both of which demonstrated features consistent with interaction with circumstellar material, were found in low-luminosity hosts (as yet undetected for SN 2002ic and $M_B = -17.4$ for SN 2005gj; Aldering et al. 2006). At the most extreme, SN 1999aw was found in a host galaxy of brightness $M_B = -11.9 \pm 0.2$ (Strolger et al. 2002). The prototype of the possible super-Chandrasekhar class, SN 2003fg, was discovered in a low luminosity galaxy whose mass was estimated at $\log(M_*/M_{\odot}) = 8.93$ (Howell et al. 2006), though it is possible this is a tidal feature of a larger morphologically-disturbed galaxy nearby.

While the prevalence of unusual SNe Ia in low-luminosity galaxies is intriguing, it is by no means a one-to-one relationship. Most of the SN 2002cx-like host galaxies are spirals of moderate stellar mass (Foley et al. 2009), and other super-Chandrasekhar candidates have been found in more massive galaxies. SN 2006gz was found in a bright Scd galaxy (Hicken et al. 2007), and SN 2009dc appeared to be located in a massive S0 galaxy but may be associated with a nearby blue companion at the same redshift which may be interacting with the fiducial host of SN 2009dc (Silverman et al. 2011; Taubenberger et al. 2010).

There have also been relatively normal SNe Ia in low luminosity galaxies. The host galaxy of SN 2006an has an extremely low luminosity ($M_g = -15.3$, SDSS) and stellar mass ($\log(M_*/M_{\odot}) = 7.7$, Kelly et al. 2010) but was matched spectroscopically to the normal SN Ia SN 1994D (Quimby et al. 2006). The Catalina Real-Time Transient Survey (Drake et al. 2009) discovered SN 2008hp in a very faint ($M_g = -12.7$) host galaxy, but matched it spectroscopically to a normal SN Ia (Drake et al. 2008). Additionally, the SNfactory discovered a number of relatively normal SNe Ia in low luminosity galaxies (Childress et al., in preparation).

To summarize, we note that low luminosity SN Ia hosts do not exclusively produce unusual SNe Ia, but there appears to be a higher frequency of these peculiar SNe Ia, including SN 2007if, in lower luminosity hosts.

6.3. Host Age Constraint - Implications for SN 2007if Progenitor Scenarios

A consistent picture for the progenitor of any supernova should be able to explain not only the energetics of the explosion itself, but also the rates and timescales of such events. For normal SNe Ia, the correlation of SN rates with host galaxy mass and star-formation rate (Mannucci et al. 2005; Sullivan et al. 2006) indicated the likelihood of two progenitor components (the “A+B” model Scannapieco & Bildsten 2005) with different time scales. This is most directly encapsulated in the SN Ia delay time distribution (DTD; Mannucci et al. 2006). While the DTD of SNe Ia is still debated (see e.g. Mennekens et al. 2010), the predictions of various scenarios for normal SNe Ia serve as a useful baseline for placing our age constraint for HOST07if in the context of progenitor scenarios for SN 2007if.

Though the presence of SNe Ia in elliptical galaxies and the decline of the SN Ia rate at high redshift argue for progenitors with long delay times (Strolger et al. 2004, 2005), the correlation of SNe Ia with star-formation indicates the need for short-lived SN Ia progenitors (Aubourg et al. 2008) with delay times of order a few hundred Myr. Such short timescales have indeed been obtained in models of SD progenitor scenarios (e.g. Hachisu, Kato, & Nomoto 2008, their WD+MS channel), and DD scenarios (e.g. Ruiter et al. 2009).

As an example, Mennekens et al. (2010) describe a particular DD channel (dubbed the “CE” channel) in which two stars, with initially large separation and orbital period of several hundred days, undergo two common-envelope phases at the end of the main sequence lifetime of the more massive star. Following the MS evolution and the CE episodes, the orbital period of the system is reduced to a few hundred seconds and rapidly decays by gravitational radiation over a few hundred kyr. Finally the two WDs merge after a total period of order a few hundred Myr from the initial birth of the stars. This binary evolution channel has delay times consistent with our age estimate for the stellar population of HOST07if.

Liu et al. (2010) proposed a stellar evolution channel for super-Chandrasekhar SNe Ia involving a CO-WD primary and He secondary. This system is born from a binary with initial masses of $M_1 = 7.5 M_\odot$ and $M_2 = 4.0 M_\odot$ (at solar metallicity) that undergoes rapid rotation and explodes as a super-Chandrasekhar SN Ia with a delay time of approximately $t_{\text{super-Ch}} \approx 65$ Myr. Though the initial masses and timescales would be different at the sub-solar metallicity of HOST07if, the timescale of this scenario is roughly the same order of magnitude as our age constraint from the host spectrum.

Blais & Nelson (2011) proposed a new binary evolution scenario which could lead to an SN Ia through the DD channel. In their “single CE” scenario, two stars of very similar mass ($M_1/M_2 > 0.95$) fill their Roche lobes almost simultaneously, leading to a common envelope episode that brings the remnant WDs to a much tighter orbital separation followed by the standard DD merger as a result of orbital energy dissipation due to gravitational radiation losses. Their scenario manifests a large range of timescales, from less than 100 Myr to greater than a Hubble time, which allows for the timescale that we estimate for the age of HOST07if. Indeed, a non-negligible fraction of the short timescale ($\log(t) \leq 8.2$) realizations of this scenario show a total WD system mass in the range $2.1 M_\odot \leq M_{\text{WD,tot}} \leq 2.3 M_\odot$ (L. Nelson, private communication), in line with the total system mass estimate we derived for SN 2007if in Scalzo et al. (2010).

Short timescales similar to the age of HOST07if are allowed in some SD scenarios [e.g. the “WD+MS” channel of Hachisu, Kato, & Nomoto (2008), see also Han & Podsiadlowski (2004), Greggio (2005) and references therein], but are especially common in DD scenarios (Yungelson & Livio 2000; Greggio 2005; Ruiter et al. 2009; Mennekens et al. 2010). While our age constraint does not definitely establish whether one of the traditional SN Ia progenitor scenarios or a new scenario is more favored for SN 2007if, our determination that SN 2007if was likely born from a young stellar population disfavors some scenarios, such as the WD+RG channel of the SD scenario from Hachisu, Kato, & Nomoto (2008) in which the WD accretes matter from a red giant companion, or the “RLOF” channel of the DD scenario described by Mennekens et al. (2010) in which early mass transfer in the binary proceeds by slow Roche lobe overflow (RLOF) and requires a significantly longer delay time than the age we measure for HOST07if.

Another interesting consequence of our age constraint is the resultant progenitor WD mass constraint for SN 2007if. If we assume SN 2007if originated from the merger of two WDs born in the dominant HOST07if starburst that have evolved off the main sequence prior to merger, we can use models connecting initial MS and final WD mass to derive a crude lower limit for the total system mass prior to SN Ia explosion. Using the models of Umeda et al. (1999a, see their Fig. 6)

at $Z = 0.004$, we roughly estimate that a $M/M_\odot = 4.6$ main sequence star (corresponding to the MS turnoff mass derived above for HOST07if) would produce a $M_{\text{WD}} = 0.85 M_\odot$ white dwarf. Thus in this toy model SN 2007if should have originated from the merger of two WDs whose total mass can be no less than $M_{\text{tot}} = 1.70 M_\odot$, clearly in excess of M_{Ch} . There must some dynamical orbital decay time for a double WD merger, so this approximation should be considered an extreme lower limit. Though the evolution of post-MS stars in binary systems is far more complicated than the single star evolutionary scenarios of Umeda et al. (1999a), these models provide a good approximate scale of the available C/O material at the time of WD merger. Thus, our age estimate for HOST07if implies that even if stars just leaving the main sequence in HOST07if merge immediately, their mass must exceed the Chandrasekhar mass by a fair margin, reinforcing the model of SN 2007if as a super-Chandrasekhar SN Ia we derived in Scalzo et al. (2010).

7. CONCLUSIONS

We have presented Keck photometry and spectroscopy of the faint host galaxy of the super-Chandrasekhar SN Ia SN 2007if. HOST07if has very low stellar mass ($\log(M_*/M_\odot) = 7.32 \pm 0.17$), and has the lowest-reported spectroscopically-measured metallicity ($12 + \log(O/H)_{\text{KK04}} = 8.01 \pm 0.09$ or $12 + \log(O/H)_{\text{T04}} = 7.71 \pm 0.14$ [stat] ± 0.06 [sys]) of any SN Ia host galaxy. We used the Balmer absorption line strengths in conjunction with the 4000Å break to constrain the age of the dominant starburst in the galaxy to be $t_{\text{burst}} = 123_{-77}^{+165}$ Myr, corresponding to a main-sequence turn-off mass of $M/M_\odot = 4.6_{-1.4}^{+2.6}$.

This host galaxy is an ideal system for measuring SN progenitor properties. Dwarf galaxies such as HOST07if typically have a well-mixed ISM, lacking the large-scale abundance gradients found in larger galaxies. Like other low-mass dwarf galaxies, HOST07if shows indications of a bursty star-formation history, as its recent star-formation is dominated by the large starburst approximately 123 Myr in its past which presumably gave birth to the progenitor system of SN 2007if. We note, however, that bright recent starbursts are efficient at obscuring the light of older stellar populations, and HOST07if could possibly have a significant amount of mass in older stars (c.f. §4.2). However, we also showed that with the decreased probability of SN 2007if arising from progressively older stars, the allowable amount of old stars in HOST07if leaves only a small probability that the SN was not born in the most recent starburst. Our constraints on the age and metallicity of the host of SN 2007if do not constitute direct constraints on the properties of its progenitor, but rather characterize the distribution of stars from which its progenitor was drawn. Nonetheless, the low metallicity and young stellar age of HOST07if are robust measurements (c.f. §5), and strengthen our interpretation that the properties of HOST07if are good indicators of the properties of the SN 2007if progenitor itself.

Our results provide key properties that should be reproduced by any proposed progenitor scenarios for SN 2007if. The low host metallicity can be used as input to stellar evolutionary tracks chosen for progenitor modeling, and will be particularly important in the mass loss stages of the progenitor. The relatively short timescale for the explosion of SN 2007if provides constraints on the binary evolution of the progenitor system. While development of a consistent pro-

genitor scenario for super-Chandrasekhar SNe Ia is beyond the scope of this work, we have shown that a key member of this subclass, SN 2007if, is very likely to have originated from a low-metallicity young progenitor. Future inspection of the hosts of other super-Chandrasekhar SNe Ia will be critical for assessing the frequency of these characteristics for super-Chandrasekhar SN Ia progenitors.

Acknowledgments: The authors would like to thank the excellent technical and scientific staff at Keck Observatory. The data presented herein were obtained at the W. M. Keck Observatory, which is operated as a scientific partnership among the California Institute of Technology, the University of California, and the National Aeronautics and Space Administration; the Observatory was made possible by the generous financial support of the W. M. Keck Foundation. We wish to recognize and acknowledge the very significant cultural role and reverence that the summit of Mauna Kea has always had within the indigenous Hawaiian community, and we are extremely grateful for the opportunity to conduct observations from this mountain. We thank Lorne Nelson and Eric Blais for insightful discussions about their SN Ia progenitor work. We would also like

to thank the anonymous referee for very constructive comments which helped improve the quality of this paper.

This work was supported by the Director, Office of Science, Office of High Energy Physics, of the U.S. Department of Energy under Contract No. DE-AC02-05CH11231; by a grant from the Gordon & Betty Moore Foundation; and in France by support from CNRS/IN2P3, CNRS/INSU, and PNC. CW acknowledges support from the National Natural Science Foundation of China grant 10903010. This research used resources of the National Energy Research Scientific Computing Center, which is supported by the Director, Office of Science, Office of Advanced Scientific Computing Research, of the U.S. Department of Energy under Contract No. DE-AC02-05CH11231. We thank them for a generous allocation of storage and computing time. HPWREN is funded by National Science Foundation Grant Number ANI-0087344, and the University of California, San Diego.

Some data used in this paper were obtained from the Sloan Digital Sky Survey (SDSS). Funding for the SDSS and SDSS-II has been provided by the Alfred P. Sloan Foundation, the Participating Institutions, the National Science Foundation, the U.S. Department of Energy, the National Aeronautics and Space Administration, the Japanese Monbukagakusho, the Max Planck Society, and the Higher Education Funding Council for England. The SDSS Web Site is <http://www.sdss.org/>.

REFERENCES

- Abazajian, K., et al., 2009, *ApJS*, 182, 543
 Akerlof, C. et al., 2007, *CBET*, 1059, 1
 Aldering, G., et al., 2002, *SpIE*, 4836, 61
 Aldering, G., et al., 2006, *ApJ*, 650, 510
 Aubourg, E., et al., 2008, *A&A*, 492, 631
 Balogh, M., et al., 1999, *ApJ*, 527, 54
 Barbary, K. et al., 2010, *arxiv:1010.5786*
 Bell, E., & de Jong, R., 2001, *ApJS*, 550, 212
 Bertin, E., & Arnouts, S. 1996, *A&AS*, 117, 393
 Bertin, E., Mellier, Y., Radovich, M., Missonnier, G., Didelon, P., & Morin, B. 2002, *Astronomical Data Analysis Software and Systems XI*, 281, 228
 Bertin, E. 2006, *Astronomical Data Analysis Software and Systems XV*, 351, 112
 Blais, E., & Nelson, L. 2011, *Bulletin of the American Astronomical Society*, 43, #324.03
 Bruzual, G., & Charlot, S., 2003, *MNRAS*, 344, 1000
 Cardelli, J., Clayton, G. & Mathis, J. 1989, *ApJ*, 345, 245
 Cardiel, N., et al., 1998, *A&AS*, 127, 597
 Chabrier, G., 2003, *PASP*, 115, 763
 Charlot, S., & Longhetti, M., 2001, *MNRAS*, 323, 887
 Conroy, C., Gunn, J. & White, M. 2009, *ApJ*, 699, 486
 Delahaye, F., et al., 2010, *arXiv:1005.0423*
 Donahue, M., Aldering, G. & Stocke, J. 1995, *ApJ*, 450, L45
 Drake, A., et al., 2009, *ApJ*, 696, 870
 Drake, A., et al., 2008, *CBET*, 1589, 1
 Foley, R., et al., 2009, *AJ*, 138, 376
 Gallazzi, A., & Bell, E., 2009 (GB09), *ApJS*, 185, 253
 Gallazzi, A., et al., 2005, *MNRAS*, 362, 41
 Garn, T. & Best, P., 2010, *MNRAS*, 409, 421
 Graves, G., & Schiavon, R., 2008, *ApJS*, 177, 446
 Greggio, L., 2005, *A&A*, 441, 1055
 Gunn, J., & Stryker, L., 1983, *ApJS*, 52, 121
 Hachisu, I., Kato, M., & Nomoto, K., 2008, *ApJ*, 679, 1390
 Hamuy, M. et al., 2000, *AJ*, 120, 1479
 Hamuy, M. et al., 2003, *Nature*, 424, 651
 Han, Z., & Podsiadlowski, P., 2004, *MNRAS*, 350, 1301
 Hanuschik, R. W., 2003, *A&A*, 407, 1157
 Hicken, M. et al., 2007, *ApJ*, 669, L17
 Hinshaw, G., et al., 2009, *ApJS*, 180, 225
 Howell, D. A. et al., 2006, *Nature*, 443, 308
 Iben, I., & Tutukov, A., 1984, *ApJS*, 54, 335
 Kauffmann, G., et al., 2003a, *MNRAS*, 341, 33
 Kelly, P. et al., 2010, *ApJ*, 715, 743
 Kennicutt, R., 1998, *ARA&A*, 36, 189
 Kennicutt, R., Bresolin, F., & Garnett, D., 2003, *ApJ*, 591, 801
 Kewley, L., & Dopita, M., 2002, *ApJS*, 142, 35
 Kewley, L., & Ellison, S., 2008, *ApJ*, 681, 1183
 Kobayashi, C., & Nomoto, K., 2009, *ApJ*, 707, 1466
 Kobulnicky, H., & Kewley, L., 2004, *ApJ*, 617, 240
 Kobulnicky, H. et al., 1999, *ApJ*, 514, 544
 Lee, J., et al., 2009, *ApJ*, 706, 599
 Leibundgut, B., 2000, *ARA&A*, 10, 179
 Liu, W.-M., et al., 2010, *A&A*, 523, 3
 Mannucci, F., et al., 2005, *A&A*, 433, 807
 Mannucci, F., et al., 2006, *MNRAS*, 370, 773
 Maoz, D., 2010, *AIPC*, 1314, 223
 McGaugh, S., 1991, *ApJ*, 380, 140
 Mennekens, N., et al., 2010, *A&A*, 515, 89
 Mink, D. 2006, *Astronomical Data Analysis Software and Systems XV*, 351, 204
 Nava, A., et al., 2006, *ApJ*, 645, 1076
 Nomoto, K., et al., 1995, *ASPC*, 72, 164
 Nugent, P., 2007, *ATEL #1213*
 Nugent, P., Kim, A., & Perlmutter, S., 2002, *PASP*, 114, 803
 Oke, J. B., et al., 1995, *PASP*, 107, 375
 Osterbrock, D. E., & Ferland, G. J. 2006, *Astrophysics of gaseous nebulae and active galactic nuclei*, 2nd. ed. by D.E. Osterbrock and G.J. Ferland. Sausalito, CA: University Science Books, 2006.
 Peebles, M., et al., 2008, *ApJ*, 685, 904
 Perlmutter, S., et al., 1999, *ApJ*, 517, 565
 Phillips, A., et al., 2007, *SpIE*, 6269, 56
 Piro, A., 2008, *ApJ*, 679, 616
 Prieto, J., et al., 2007, *arxiv:0706.4088*
 Prieto, J., Stanek, K., & Beacom, J., 2008, *ApJ*, 673, 999
 Quimby, R., et al., 2006, *CBET*, 413, 1
 Raskin, C., et al., 2010, *ApJ*, 724, 111
 Riess, A., et al., 1998, *AJ*, 116, 1009
 Ruiter, A., et al., 2009, *ApJ*, 699, 2026
 Salpeter, E. E., 1955, *ApJ*, 121, 161
 Sánchez Almeida, J., et al., 2008, *ApJ*, 685, 194
 Sánchez Almeida, J., et al., 2009, *ApJ*, 698, 1497
 Scalzo, R., et al., 2010, *ApJ*, 713, 1073
 Scannapieco, E., & Bildsten, L., 2005, *ApJ*, 629, 85
 Schechter, P., 1976, *ApJ*, 203, 297
 Schlegel, D. J., Finkbeiner, D. P. & Davis, M., 1998, *ApJ*, 500, 525
 Searle, L., & Sargent, W., 1972, *ApJ*, 173, 25
 Silverman, J. M. et al., 2011, *MNRAS*, 410, 585
 Skrutskie, M., et al., 2006, *AJ*, 131, 1163
 Stoughton, C., et al., 2002, *AJ*, 123, 485
 Strolger, L., et al., 2002, *AJ*, 124, 2905
 Strolger, L., et al., 2004, *ApJ*, 613, 200
 Strolger, L., et al., 2005, *ApJ*, 635, 1370
 Sullivan, M., et al., 2006, *ApJ*, 648, 868
 Tanaka, M., et al., 2010, *ApJ*, 714, 1209
 Taubenberger, S. et al., 2010, *arXiv:1011.5665*
 Tremonti, C., et al., 2004, *ApJ*, 613, 898
 Umeda, H., et al., 1999a, *ApJ*, 513, 861
 Umeda, H., et al., 1999b, *ApJ*, 522, L43
 van Dokkum, P., 2001, *PASP*, 113, 1420
 Vazdekis, A., et al., 2010, *MNRAS*, 404, 1639
 Whelan, J., & Iben, I., 1973, *ApJ*, 186, 1007
 Wood-Vasey, M., et al., 2002, *IAUC*, 7842, 1
 Wood-Vasey, M., Wang, L. & Aldering, G. 2004, *ApJ*, 616, 339
 Worthey, G., et al., 1994, *ApJS*, 94, 687
 Worthey, G., & Ottaviani, D., 1994, *ApJS*, 111, 377
 Wright, N., 2006, *PASP*, 118, 1711
 Yamanaka, M. et al., 2009, *ApJ*, 707, L118
 York, D., et al., 2000, *AJ*, 120, 1579
 Yuan, R., et al., 2010, *ApJ*, 715, 1338
 Yungelson, L., & Livio, M., 2000, *ApJ*, 528, 108

Zaritsky, D., et al., 1994, ApJ, 420, 87
Zhao, Y., Gu, Q., & Gao, Y., 2011, AJ, 141, 68